Electronic Supplementary Material (ESI) for New Journal of Chemistry.

Polyaniline-zeolite nanocomposite material based acetylcholinestrase biosensor for the sensitive detection of acetylcholine and organophosphates

Balwinder Kaur and Rajendra Srivastava*

Supporting Information

Synthesis Mechanism for PANI-Nano-ZSM-5

PANI-Nano-ZSM-5 hybrid material was synthesized by the oxidative polymerization of aniline with ammonium peroxydisulfate (APS) in an aqueous zeolite suspension by the in-situ surface polymerization method. Nano-ZSM-5 was first surface functionalized with propyl amine group to favor the growth of PANI film on the surface of Nano-ZSM-5 and not in the bulk solution. P123 is a neutral polymeric surfactant and is used to prepare a variety of mesostructured materials.[1, 2] P123 is amphiphilic and non ionic surfactant and it can form polymer coils in aqueous solution under a dilute concentration.[3] P123 macromolecules could be attached on the peripheral amine groups of Nano-ZSM-5 nanoparticles through hydrogen bonding. Sodium dodecyl sulfate (SDS) was subsequently added to the solution, which could form a double surfactant layer with negative polar head group of SDS molecule. Aniline monomers could form cationic anilinium ions (An^+) under acidic condition. An^+ could adsorb on the surface of Nano-ZSM-5 with electrostatic interaction with double surfactant layer. Upon the addition of APS, PANI nucleation could takes place that are stabilized by the P123/SDS double surfactant layer attached on Nano-ZSM-5 surface.[4] The polymerization usually takes place preferentially and continuously in proximity to existing PANI. Hence, the polymerization was initiated, propagated, and terminated on the surface of Nano-ZSM-5, rather than in bulk solution. Therefore, PANI film was formed on the surface of Nano-ZSM-5.

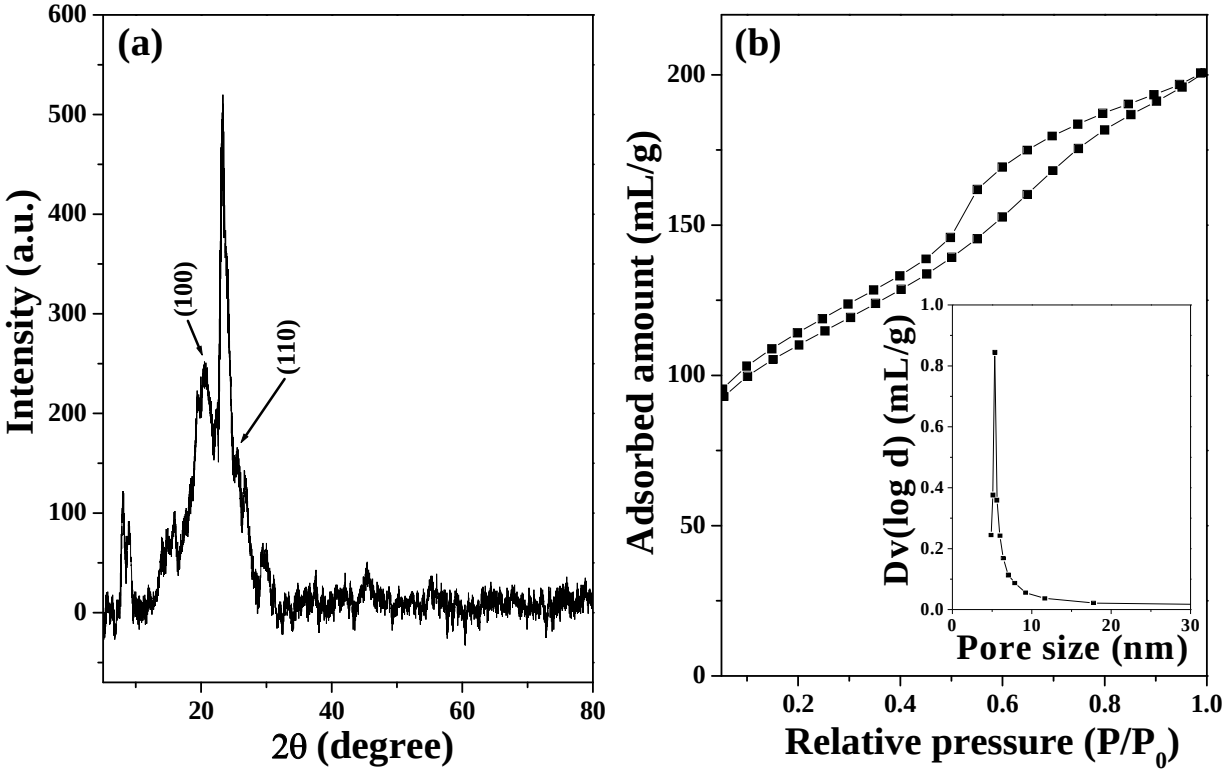

Fig. S1. (a) XRD pattern (plane shown here represent the incorporation of PANI in the nanocomposite, remaining XRD diffraction corresponds to Nano-ZSM-5) and (b) N_2-adsorption isotherm of PANI-Nano-ZSM-5 nanocomposite material (inset shows pore size distribution).

The XRD pattern of PANI-Nano-ZSM-5 exhibited the diffraction peaks corresponding to both, PANI and Nano-ZSM-5, phases. The N_2-adsoption isotherm for PANI-Nano-ZSM-5 exhibited type-IV isotherm similar to that of mesoporous materials. The mesopores for PANI-Nano-ZSM-5 showed a narrow pore size distribution (5-8 nm). The total surface area, external surface area and total pore volume for PANI-Nano-ZSM-5 was found to be 297 m^2/g, 123 m^2/g, and 0.41 cm^3/g, respectively.

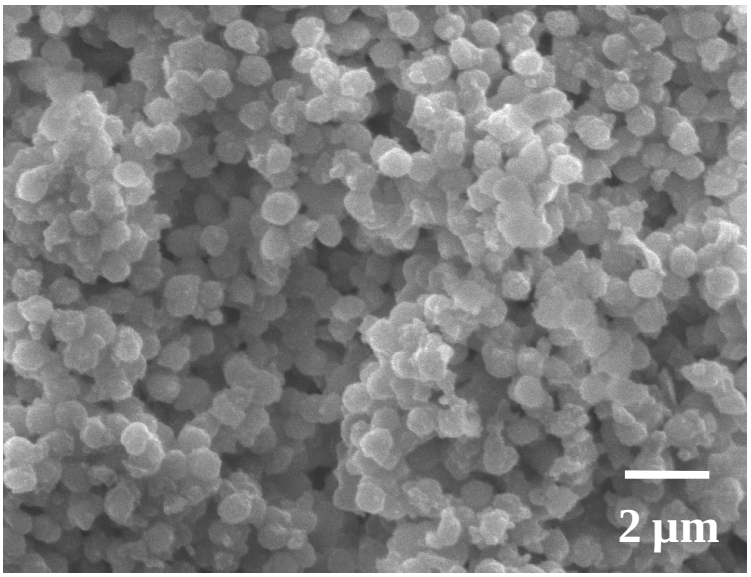

Fig. S2. SEM image of PANI-Nano-ZSM-5 nanocomposite.

The SEM image confirmed that PANI film was formed on the surface of spherical Nano-ZSM-5 particles. SEM image also confirmed that no separate phase for bulk PANI was observed.

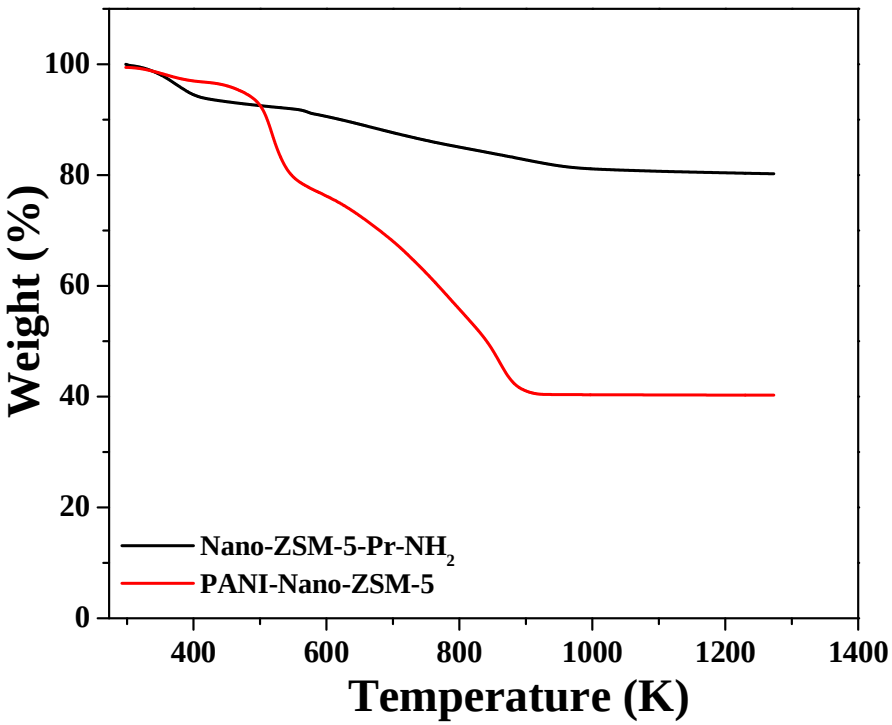

Fig. S3. TGA thermograms of Nano-ZSM-5-Pr-NH_2, and PANI-Nano-ZSM-5 materials at a heating rate of 10 K/min recorded in air stream.

The first weight loss below 473 K in the TGA curves for the samples indicates the loss of physically adsorbed water molecules. In the TGA curve for Nano-ZSM-5-Pr-NH_2, the second weight loss between 525-875 K can be attributed to the decomposition of organic propylamine moiety anchored on the surface of Nano-ZSM-5 and the residual weight refers to the content of Nano-ZSM-5 in Nano-ZSM-5-Pr-NH_2. TGA analysis confirmed that Nano-ZSM-5-Pr-NH_2 contains 11 wt % functionalized organic group (-Pr-NH_2). In the TGA curve for PANI-Nano-ZSM-5, the combustion of PANI in air stream was completed at 913 K and the residual weight refers to the content of Nano-ZSM-5 in the nanocomposite. TGA confirms that PANI-Nano-ZSM-5 nanocomposite contains 40.7 wt % Nano-ZSM-5 and 43.8 wt % PANI. Nano-ZSM-5/PANI weight ratio was found to be 0.93, which was very close to their initial weight ratio.

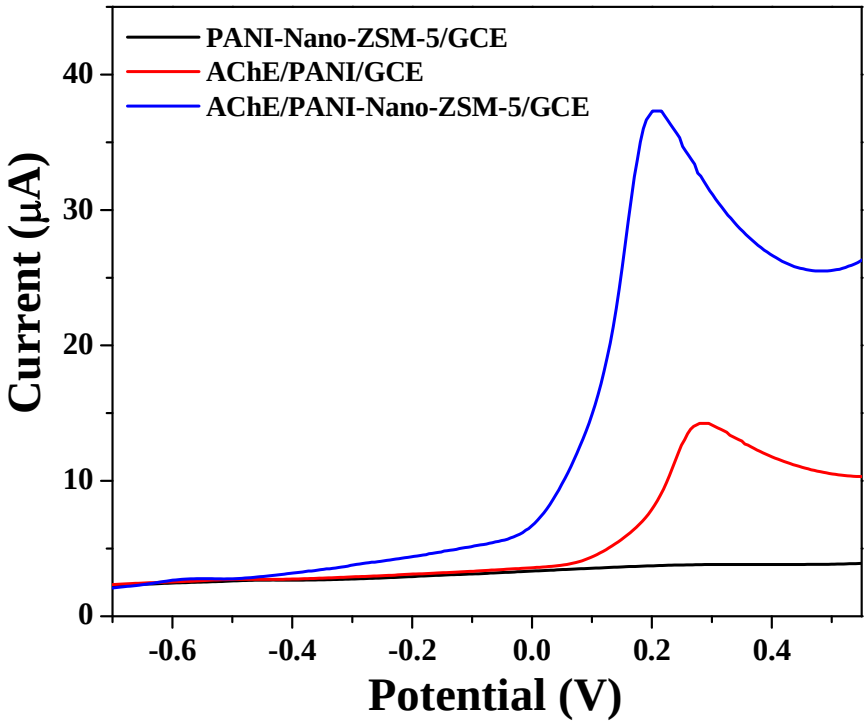

Fig. S4. SWVs at different modified electrodes (PANI-Nano-ZSM-5/GCE, AChE/PANI/GCE, and AChE/PANI-Nano-ZSM-5/GCE) in 0.002 M PBS containing 0.1 M NaCl (pH 7.4) in the presence of 1 mM ACh.

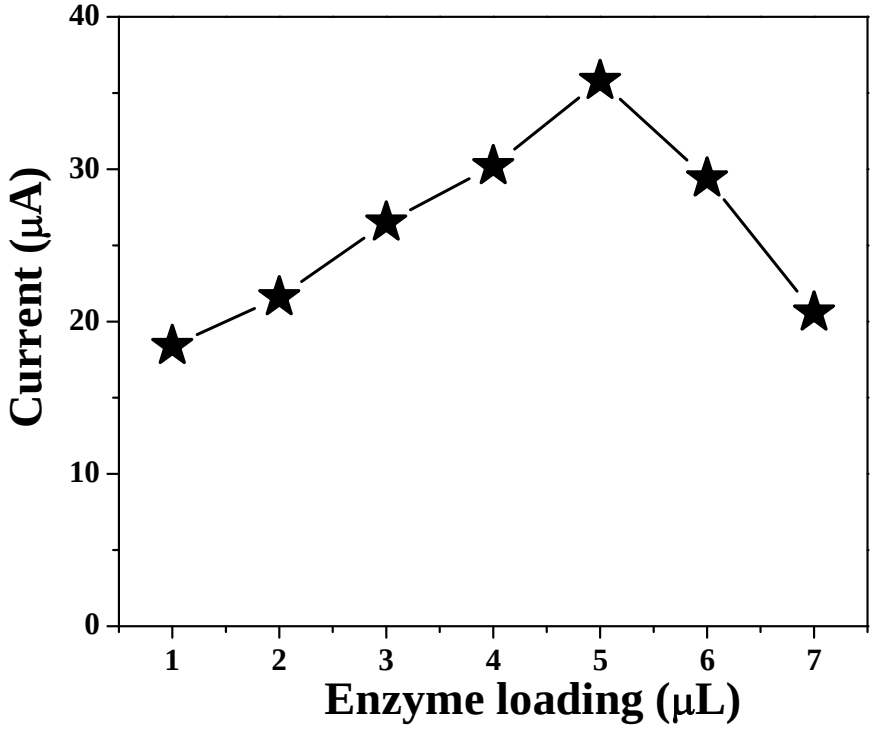

Fig. S5. Influence of enzyme loading on AChE/PANI-Nano-ZSM-5/GCE biosensor response in the presence of 1 mM ACh.

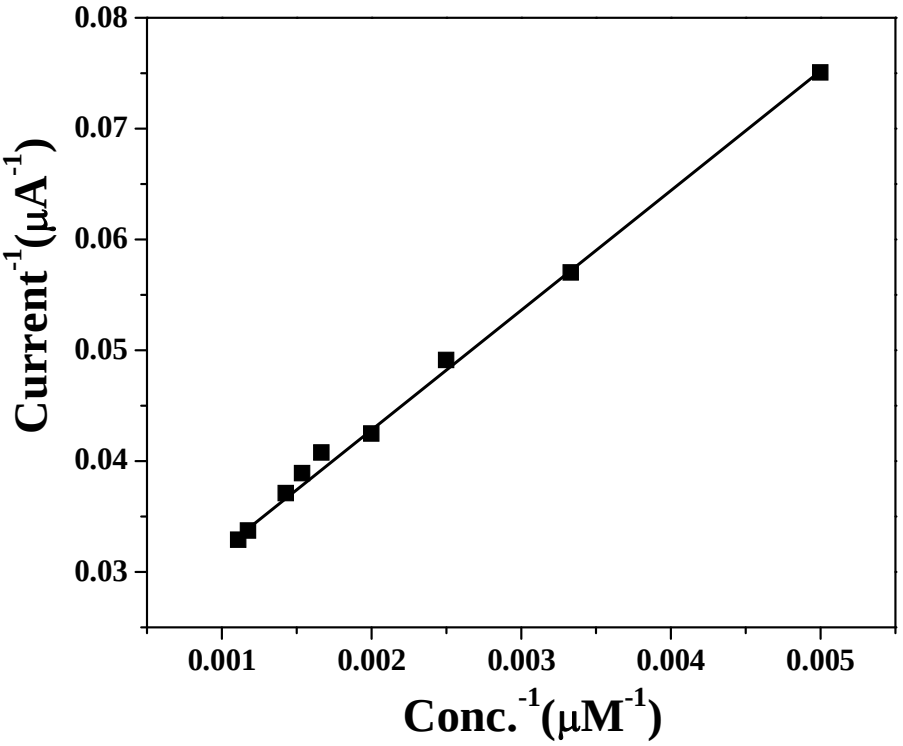

Fig. S6. Lineweaver-Burk plot for amperometric response of AChE/PANI-Nano-ZSM-5/GCE biosensor toward ACh addition.

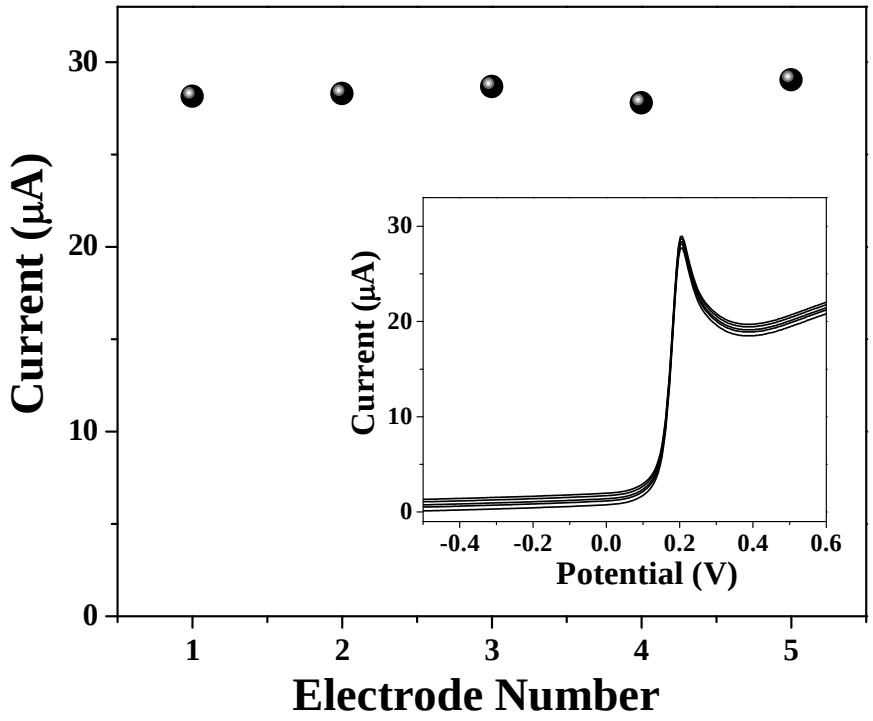

Fig. S7. The current response at different freshly prepared AChE/PANI-Nnao-ZSM-5/GCEs (n=5) after being immersed in 50 ppb monocrotopos for 5 min. Inset shows corresponding SWV response at 5 different AChE/PANI-Nnao-ZSM-5/GCEs in the presence of 1 mM ACh in 0.002 M PBS containing 0.1 M NaCl (pH 7.4) after being immersed in 50 ppb monocrotopos for 5 min.

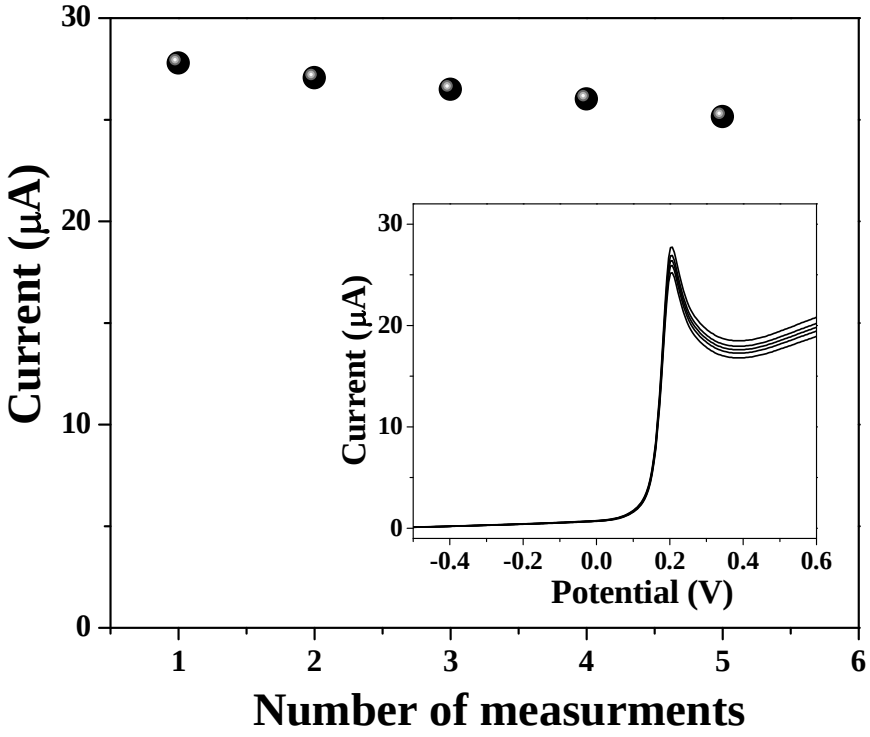

Fig. S8. The current response at five different measurements using same AChE/PANI-Nano-ZSM-5/GCE after being immersed in 50 ppb monocrotopos for 5 min. Inset shows corresponding SWV response at 5 different measurements using same AChE/PANI-Nano-ZSM-5/GCE in the presence of 1 mM ACh in 0.002 M PBS containing 0.1 M NaCl (pH 7.4) after being immersed in 50 ppb monocrotopos for 5 min.

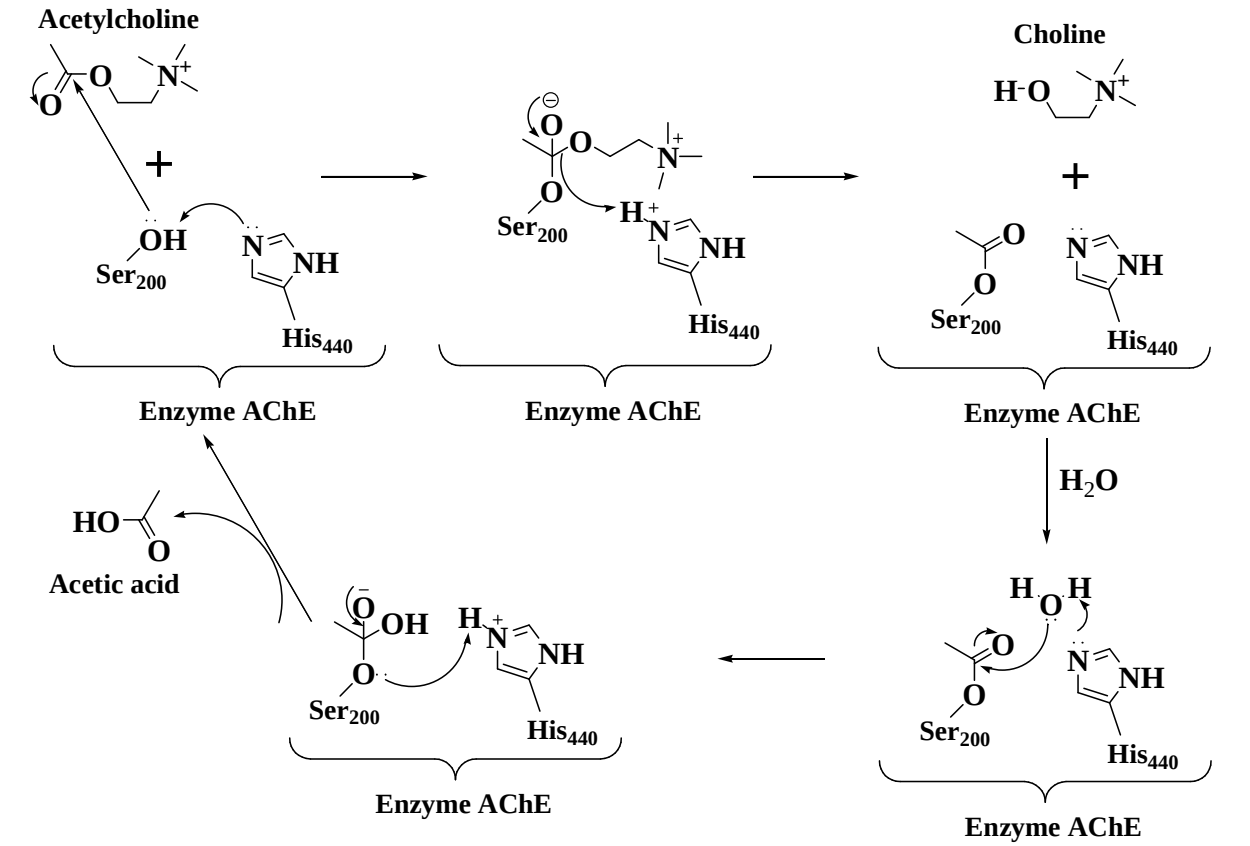

Scheme S1a

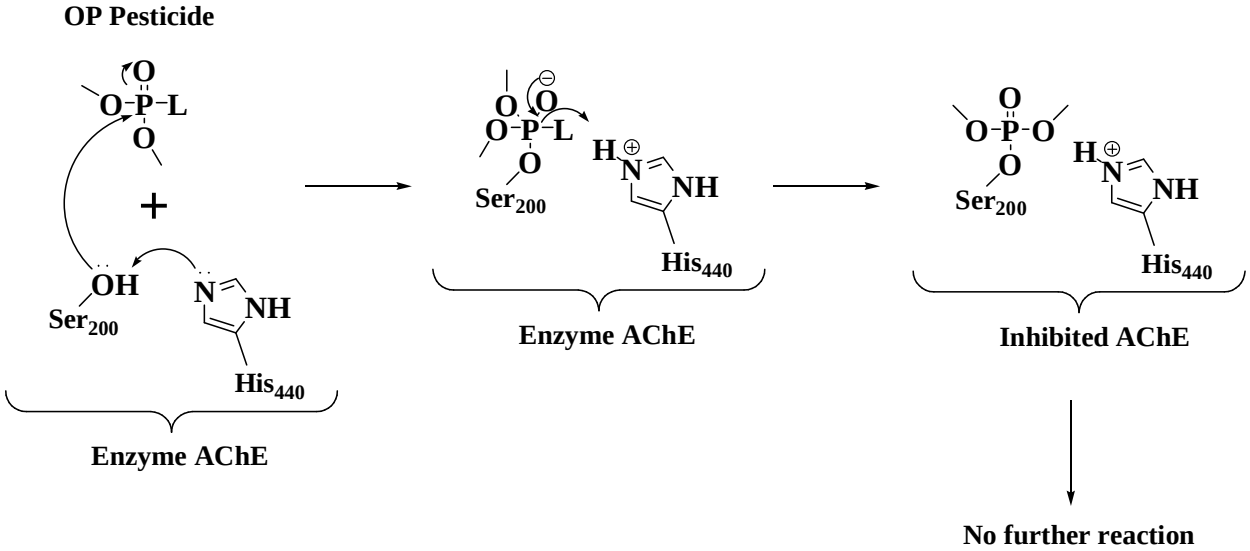

Scheme S1b

Scheme S1. (a) Hydrolysis of acetylcholine by enzyme AChE and (b) Inhibition of enzyme AChE by organophosphate pesticides (OP) at AChE/PANI-Nano-ZSM-5/GCE biosensor.

Table S1. Comparison of AChE/PANI-Nano-ZSM-5/GCE biosensor with other biosensors reported in the literature for OP detection.

S.No.	Modified electrode	OP pesticide	Linear range (ppb)	Detection limit (ppb)	Michaelis-Menten constant	Reference
1.	ZnO-AChE	paraoxon	35 – 1380	35	-	[5]
2.	AChE-TiO_2-G/GCE	carbaryl	1 – 15	0.3	220 µM	[6]
3.	AChE-PAn-PPy-MWCNTs/GCE	Malathion	10 – 500	1	-	[7]
4.	AChE/PBNCs/rGO	monocrotophos	1 – 600	0.1	-	[8]
5.	AChE/gold nanoparticle/sol–gel	Monocrotophos	0.1 – 1000	0.6	450 µM	[9]
6.	AChE-AuNP–polypyrrole nanowires	Methyl parathion	5 – 120	2	-	[10]
7.	Au–TiO_2/chitosan	Parathion	1 – 7000	0.5	-	[11]
8.	PPy-AChE-Geltn-Glut/Pt	Paraoxon	12.5 – 150	1.1	2 mM	[12]
9.	CdTe/gold nanoparticles modified chitosan microspheres	Monocrotophos	1 – 1000	0.3	-	[13]
10.	MWCNT for solid-phase extraction	Methyl parathion	50 – 2000	5	-	[14]
11.	AChE–Er-GRO–Nafion/GCE	dichlorvos	5 – 100	2	700 µM	[15]
12.	AChE-MWCNTs-Au-CHIT/GCE	malathion	1 – 1000	0.6	268 µM	[16]
13.	AChE/PANI-Nano-ZSM-5/GCE	Monocrotopos Dichlorvos	1 -1000 3 - 1000	0.1 0.2	232 µM	This work

Table S2. The electro-catalytic response of AChE/PANI-Nano-ZSM-5/GCE biosensor toward the detection of different OP pesticides.

S.No.	OP pesticide	Linear range (ppb)	Detection limit (ppb)	Inhibition time (min)	Reactivation time (min)
1.	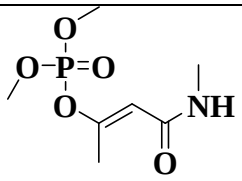 Monocrotopos	1 - 1000	0.1	5	7
2.	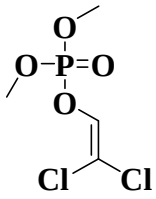 Dichlorvos	3 - 1000	0.2	5	7

References

1. M. U. Anu Prathap, B. Kaur and R. Srivastava, *J. Colloid Interface Sci.*, 2012, **381**, 143-151.
2. M. U. Anu Prathap, B. Thakur, S. N. Sawant and R. Srivastava, *Colloids Surf., B*, 2012, **89**, 108-116.
3. P. Alexandridis and T. A. Hatton, *Colloids Surf., A*, 1995, **96**, 1-46.
4. S. Xuan, Y.-X. J. Wang, K. C.-F. Leung and K. Shu, *J. Phys. Chem. C*, 2008, **112**, 18804-18809.
5. R. Sinha, M. Ganesana, S. Andreescu and L. Stanciu, *Anal. Chim. Acta*, 2010, **661**, 195-199.
6. K. Wang, H.-N. Li, J. Wu, C. Ju, J.-J. Yan, Q. Liu and B. Qiu, *Analyst*, 2011, **136**, 3349-3354.
7. D. Du, X. Ye, J. Cai, J. Liu and A. Zhang, *Biosens. Bioelectron.*, 2010, **25**, 2503-2508.
8. L. Zhang, A. Zhang, D. Du and Y. Lin, *Nanoscale*, 2012, **4**, 4674-4679.
9. D. Du, S. Chen, J. Cai and A. Zhang, *Biosens. Bioelectron.*, 2007, **23**, 130-134.
10. J. Gong, L. Wang and L. Zhang, *Biosens. Bioelectron.*, 2009, **24**, 2285-2288.
11. Y. Qu, H. Min, Y. Wei, F. Xiao, G. Shi, X. Li and L. Jin, *Talanta*, 2008, **76**, 758-762.
12. R. R. Dutta and P. Puzari, *Biosens. Bioelectron.*, 2014, **52**, 166-172.
13. D. Du, S. Chen, D. Song, H. Li and X. Chen, *Biosens. Bioelectron.*, 2008, **24**, 475-479.
14. D. Du, M. Wang, J. Zhang, J. Cai, H. Tu and A. Zhang, *Electrochem. Commun.*, 2008, **10**, 85-89.
15. S. Wu, F. Huang, X. Lan, X. Wang, J. Wang and C. Meng, *Sens. Actuators, B: Chem.*, 2013, **177**, 724-729.
16. D. Du, M. Wang, J. Cai, Y. Qin and A. Zhang, *Sens. Actuators, B: Chem.*, 2010, **143**, 524-529.